

Modelling Postbuckling Composite Structures

B. G. Falzon¹ & M. Cerini¹

Summary

This paper presents a finite element procedure for modelling the behaviour of postbuckling structures undergoing mode-switching. The arc-length method is combined with an explicit pseudo-dynamic algorithm and the routine automatically switched between these two algorithms, based on changes detected in the factored tangential stiffness matrix.

Introduction

Numerous experimental investigations of stiffened composite panels loaded in uniaxial compression have shown their load carrying capability beyond the initial skin-buckling load [1-3]. By allowing certain structural components to buckle between the design limit and ultimate loads, and in some cases even below the design limit load, significantly lighter structures may be achieved. Buckling in stiffened composite aerostructures gives rise to a dramatic increase in the interlaminar stresses at the skin-stiffener interface which are only resisted by the relatively weak through-thickness strength at these interfaces. Damage initiation and progression in these vulnerable regions is still difficult to predict and this has resulted in conservative composite designs in aerostructures.

The postbuckling behaviour of stiffened composite structures is further complicated by the observed phenomenon of mode-switching where a postbuckled panel will dynamically snap to a higher mode-shape. The I-stiffened panel shown in Figure 1, for example, was loaded in uniaxial compression until failure. Initial buckling was characterised by five half-waves in the skin bays and a dynamic mode-switch to six half-waves was observed at a loading of 240 kN followed by a further mode-switch in the outer skin-bays to seven half-waves at a loading of 487 kN. The panel failed catastrophically at a loading of 525 kN. Experimental evidence has shown that damage initiates at either a buckling node or an anti-node line [1-4]. Mode-switching results in sudden shifts in these critical locations and may even release enough energy to cause damage. Hence analytical tools used to predict structural response must be able to capture this phenomenon.

The arc-length method has been shown to be able to capture mode-switching under certain circumstances but it is by no means robust [5]. A more effective strategy is to use a combined static-dynamic analysis for modelling this behaviour and this was demonstrated by Riks *et. al* [6]. In this study, as in most that are currently

¹ Imperial College London, Department of Aeronautics, South Kensington Campus, London, SW7 2AZ, UK.

available in the literature, the switching from one solution procedure to the other is performed interactively using restarting schemes available in most finite element packages.

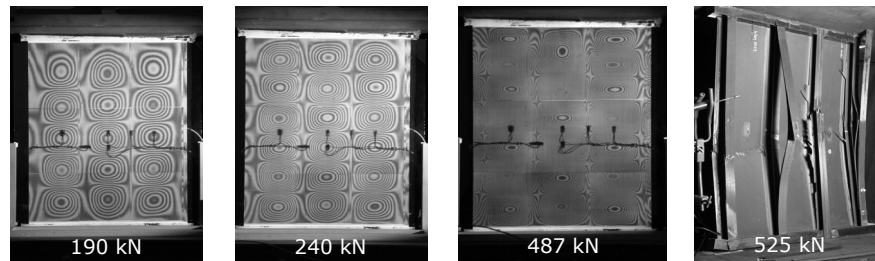


Figure 1: Moiré fringe patterns of an I-stiffened postbuckling panel

In this paper an automated static-dynamic procedure is presented. The static part of the solution process uses the arc-length constraint and a modified explicit dynamic routine, which is more computationally efficient than standard implicit and explicit dynamic schemes, is used for the transient phase. Bracketing procedures for determining the location of critical points along an equilibrium path and eigenmode injection to switch to a secondary path were also incorporated in the algorithm. This negated the need of introducing imperfections in the panel to reduce bifurcation points to limit points. This is usually done to allow arc-length routines to proceed past these critical regions but assumes that if a mode-jump occurs, the pre- and post-jump stable equilibrium paths are statically connected by an unstable equilibrium path. As pointed out by Riks [6], this is not necessarily the case and hence path-following procedures are liable to fail.

Numerical Scheme

The governing quasi-static non-linear equilibrium equations may be expressed as:

$$\mathbf{g}(\mathbf{u}, \lambda) = \mathbf{q}_i(\mathbf{u}) - \lambda \mathbf{q}_e \quad (1)$$

where $\mathbf{g}(\mathbf{u}, \lambda)$ is the vector of residual forces, $\mathbf{q}_i(\mathbf{u})$ is the vector of internal forces, \mathbf{q}_e is a fixed external load vector and λ is a load parameter. The arc-length method uses an incremental constraint which is a function of both the incremental displacements and load increment:

$$\Delta \mathbf{u}_{i+1}^T \Delta \mathbf{u}_{i+1} + \psi^2 \Delta \lambda_{i+1}^2 \mathbf{q}_e^T \mathbf{q}_e = \Delta \mathbf{u}_i^T \Delta \mathbf{u}_i + \psi^2 \Delta \lambda_i^2 \mathbf{q}_e^T \mathbf{q}_e = \dots \Delta l^2 \quad (2)$$

$\Delta \mathbf{u}_{i+1}$ and $\Delta \lambda_{i+1}$ are the incremental displacements and load, respectively, after the i th iteration and ψ is a scaling parameter. Crisfield [7] advocated setting ψ to zero

since the loading terms were shown to have little effect in practice. The iterative change in displacement is expressed as the sum of two parts: one corresponding to the iterative change that would arise out of a standard Newton-Raphson scheme and the other as the product of the load increment, $\delta\lambda$, and the displacement corresponding to a fixed external load vector. This yields a quadratic in $\delta\lambda$ and it follows that two solutions are possible. The choice of the correct load increment, notably at the start of the increment (the predictor solution), is central to this method's effectiveness. Various strategies have been proposed in the literature for determining the correct sign of $\delta\lambda$ for the predictor solution to avoid the solution from doubling-back on itself [5] but these methods have been shown to encounter difficulties in the presence of bifurcation points or sharp limit points.

Mode-Switching is a transient dynamic event and it is therefore not surprising that the use of continuation methods, such as the arc-length method outlined above, often lead to difficulty. In modelling postbuckling stiffened composite structures undergoing mode-switching, we are often only interested in locating a stable post-mode-switching equilibrium path without the need of accurately representing the behaviour during the transient phase. A modified explicit procedure is proposed [8] which aims to solve a first order explicit pseudo-dynamic equation where the damping matrix is replaced by an estimate of the tangent stiffness matrix \bar{K}_t^{-1} :

$$\dot{u}_{t+1} = \bar{K}_t^{-1} (q_e - K_t u_t) \quad (3)$$

The velocity is assumed to vary linearly over the time-step. \bar{K}_t^{-1} is computed at the start of this transient phase and will be equal to K_t and $K_t u_t$ represents the internal load vector. Once the displacements are calculated for a given load increment and time-step, a check for convergence is made and if the out-of-balance norm is above the set tolerance the solution process is advanced to the next time-step. If the ratio of this norm and that for the previous time step is greater than 1.2, \bar{K}_t^{-1} is updated. This ratio was chosen arbitrarily and may be changed by the user.

An automated static-dynamic procedure was developed for the modelling of postbuckling structures. The arc-length method is invoked while the response is quasi-static, characterised by a positive definite stiffness matrix. Using an L^TDL decomposition for the stiffness matrix K_t , where L is a lower triangular matrix and D a diagonal matrix, a positive definite matrix will have all diagonal terms in D greater than zero. When a critical point is passed, a negative diagonal term will result. At this point in the analysis, a 'bracketing procedure' is used to determine the location of this critical point more accurately. Once this has been located with sufficient accuracy, the load increment which is just above this point is used to initiate the transient phase of the analysis. To assist the solution in seeking the correct secondary path, use is made of eigenmode injection. Close to this critical

point, the eigenvalue, λ_C , will be nearly zero and the corresponding eigenvector, v_C , is scaled and used as the displacement increment. It is worth noting that while eigenvalue extraction for large problems is computationally expensive, it was recently shown [9] that λ_C and v_C may be extracted directly from the L^TDL decomposition of K_T :

$$\lambda_C = \frac{(d_{ii})_{min}}{|l_i|^2} \quad v_C = \frac{l_i}{|l_i|} \quad (4)$$

where $(d_{ii})_{min}$ is the smallest diagonal entry in D and l_i is the corresponding column of $(L^T)^{-1}$. This transient phase is stepped through time until convergence is reached within a set tolerance and then the solution procedure switches back to the arc-length method. By identifying the critical points directly and using eigenmode injection, there is no longer the need to introduce initial imperfections into the geometry to reduce bifurcation points to limit points in the hope that continuation methods will be able to represent the structural response. The nature of the critical point may be deduced by noting that $v_C^T q_e = 0$ for a bifurcation point and a non-dimensional current stiffness parameter κ , which relates the current stiffness to the initial stiffness may be used to indicate a limit point as $\kappa \rightarrow 0$.

Numerical Examples

Example 1: This method is demonstrated by the example of a beam on a non-linear elastic foundation as shown in Figure 2. Under axial compression, this beam is observed to undergo several mode-switches and serves as a good test for assessing the robustness and efficiency of the algorithm.



Figure 2: Beam on a non-linear elastic foundation.

Figure 3 shows a comparison of different numerical schemes for capturing the response of this structure and a comparison of CPU times is given in Table 1.

Table 1: CPU time (in seconds) for a beam on a non-linear elastic foundation.

No. of Elements	Arc-Length	Modified Explicit	Full Implicit	Full Explicit	Static-Dynamic
10	***	3.641	1.953	77.766	0.797
20	1.438	5.703	5.344	311.064	1.516
40	3.359	8.594	9.625	1244.256	3.328
80	4.141	12.719	27.562	4977.024	4.469
160	6.141	28.656	112.062	19631.328	7.797
320	9.266	38.578	662.047	78525.312	15.547

*** denotes convergence difficulties

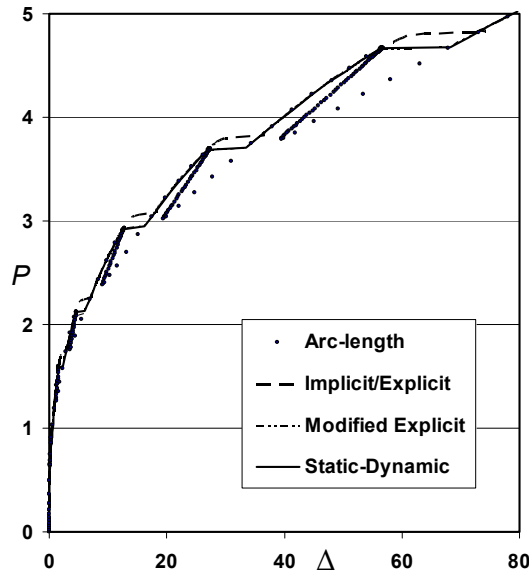


Figure 3: Load vs end-displacement for beam on a non-linear elastic foundation showing mode-switches.

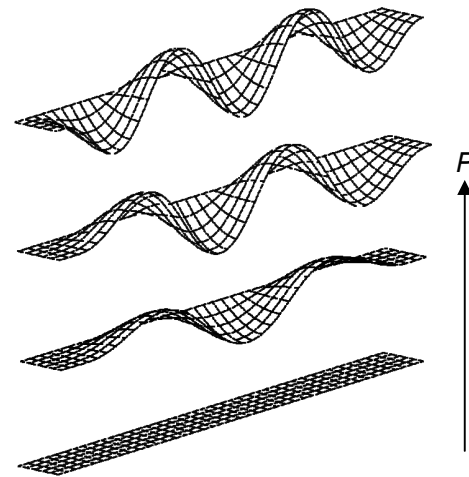


Figure 4: Deformation of aluminium skin-bay with increasing load showing mode-switches,

Example 2: A seminal experimental study by Stein [10] investigated the behaviour of a rectangular aluminium plate, subdivided into eleven skin bays and loaded in uniaxial compression. These results have been used by numerous investigators as a benchmark for validating analytical/numerical methods. A skin-bay was modelled using the present algorithm. Material non-linearity was not accounted for and the unloaded edges were fixed from moving in-plane. These boundary conditions differed from those in the actual test where the central skin-bay, in which attention was focused, had unloaded edges which remained straight but allowed to move in-plane. Figure 4 shows the first three mode-switches (3 – 4 – 5 half-waves) using the present analysis. Mode-switching is highly sensitive to boundary conditions and the first three mode-shapes reported in the experiment were (4 – 5 – 6 half-waves). The panel underwent plastic deformation at higher mode-switches.

Concluding Remarks

A robust and efficient algorithm for capturing the postbuckling behaviour of structures undergoing secondary instabilities has been presented. This method requires no user-intervention, such as restart schemes, to capture this phenomenon. By using a bracketing procedure to locate critical points and followed by

eigenmode injection to ‘point’ the displacement increment in the right direction, no initial imperfections need to be introduced in the initial geometry.

The example of the beam on a non-linear elastic foundation showed that this method was able to capture numerous mode-switches and was computationally more efficient than the full dynamic routines. While the arc-length routine was shown to be the most computationally efficient, convergence difficulties were encountered for one of the test-cases. The second example of the aluminium skin-bay, loaded in uniaxial compression, shows that the method had no difficulty in capturing mode-switching for plated structures and work is currently underway for the modelling of full stiffened composite panels.

References

1. Falzon, B.G., Stevens, K.A. and Davies, G.A.O. (2000): “Postbuckling behaviour of a blade-stiffened composite panel loaded in uniaxial compression”, *Composites Part A: applied science and manufacturing*, 31, pp. 459-468.
2. Falzon, B.G. (2001): “The behaviour of damage tolerant hat-stiffened composite panels loaded in uniaxial compression”, *Composites Part A: applied science and manufacturing*, 32, pp. 1255-1262.
3. Falzon, B.G. and Steven, G.P. (1997): “Buckling mode transition in hat-stiffened composite panels loaded in uniaxial compression”, *Composite Structures*, 37, pp. 253-267.
4. Stevens, K.A., Ricci, R., Davies, G.A.O. (2001): “Buckling and postbuckling of composite structures”, *Composites*, 26(3), pp. 189-199.
5. Cerini, M., Falzon, B.G. (2003): “The reliability of the arc-length method in the analysis of mode-jumping problems”, *44th AIAA/ASME/ASCE/AHS Structures, Structural Dynamics and Materials Conference*, Paper AIAA 2003-1621, 7-10 April, Norfolk, Virginia, USA.
6. Riks, E., Rankin, C.C., Brogan, F.A. (1996): “On the solution of mode jumping phenomenon in thin-walled structures”, *Computational Methods in Applied Mechanics and Engineering*, 136, pp. 59-92.
7. Crisfield, M.A. (1981): “A fast incremental/iterative solution of snapping and buckling problems”, *Computers and Structures*, 13, pp. 55-62.
8. Falzon, B.G., Hitchings, D. (2003): “Capturing mode-switching in postbuckling composite panels using a modified explicit procedure”, *Composite Structures*, 60, pp. 447-453.
9. Fujii, F., Noguchi, H. (2002): “The buckling mode extracted from the LDL^T-decomposed larger-order stiffness matrix”, *Communications in Numerical Methods in Engineering*, 18, pp. 459-467.
10. Stein, M. (1959): “Loads and deformations of buckled rectangular plates”, NASA Technical Report R-40.